Scientific Research Publishing

Journal of Applied Mathematics and Physics, 2026, 14(9), 3311-3330
https://www.scirp.org/journal/jamp
ISSN Online: 2327-4379
ISSN Print: 2327-4352

Mathematical Modelling of the Impact of Misdiagnosis on Dengue-Malaria Co-Infection Dynamics

Eyaran Wilson Ewesit*, Mary Wainaina, Damian Maingi

Department of Mathematics and Actuarial Science, Catholic University of Eastern Africa, Nairobi, Kenya
Email: *ewesitwilson@gmail.com

How to cite this paper: Ewesit, E.W., Wainaina, M. and Maingi, D. (2026) Mathematical Modelling of the Impact of Misdiagnosis on Dengue-Malaria Co-Infection Dynamics. *Journal of Applied Mathematics and Physics*, **14**, 3311-3330.
https://doi.org/10.4236/jamp.2026.149165

Received: August 7, 2026
Accepted: September 6, 2026
Published: September 9, 2026

Abstract

Malaria and dengue fever are among the leading causes of Undifferentiated Febrile Illness (AUFI) which account for majority visits to the hospital in Africa. The diseases are spread through biting of mosquitoes making coifection a very common phenomena in tropical and subtropical regions due to high prevalence of mosquito populations. A common challenge of managing both diseases in Africa is misdiagnosis of dengue fever for malaria due to similarities in symptoms and limited resources for accurate diagnosis. This research focused on developing a mathematical epidemiological model to investigate the impact of misdiagnosis of dengue fever as malaria on the general spread dynamics of malaria and dengue fever. The analytical properties of the spread dynamics were studied. The model was determined to be mathematically well stated and biologically well posed by ensuring the positivity and boundedness of the solutions. The co-infection-free Equilibrium was determined to exist using the jacobian matrix method. The co-infection reproductive number was calculated using the next generation matrix approach. The existence of the endemic equilibrium was determined. The normalized forward approach was used to determine the sensitivity indices and identified the parameters that most likely to be targeted for control of the malaria-dengue fever coinfection spread dynamics. Numerical simulations were conducted to obtain the numerical values of the sensitivity analysis and the numerical solutions to the spread dynamics.

Keywords

Basic Reproductive Number, Coinfection Dynamics, Malaria-Dengue Fever, Equilibrium Points, Mathematical Modelling, Numerical Simulations

1. Introduction

The monoinfection of either malaria or dengue fever by itself is fatal, however, the coinfection of both diseases has been proven to be more fatal [1]. Since they are both spread by mosquitoes, their prevalence in Africa has become more prevalent [2]. The two diseases even share common signs such as fever, headache, myalgia, nausea, and diarrhoea. As a consequence, the coinfection of the diseases is either ignored or leads to misdiagnosis of coinfection as malaria since malaria is more pronounced when compared to dengue fever [3]. In resource limited countries such as Kenya, the probability of presumptive treatment of dengue fever as malaria is very high [4].

More so, coinfection is often is treated as a mono infection due to the clinical similarities in the manifestation of the disease. Misdiagnosis is more prone in coinfection spread dynamics than in regions that have a prevalence of one disease. Concurrent infection often occurs and obscures the symptoms of either of the initial conditions and the treatment regime of coifection is not the same as the treatment of the mono infection of either disease. As a result, the delayed implementation of the correct treatment regime leads to complications that can be fatal [5]. Increased movement of populations arising from efficient transport systems is posed to further aggravate the situation by introducing the disease to new environments where the diseases were not prevalent leading to further coinfection.

Malaria and dengue are the leading causes of Acute Undifferentiated Febrile Illness (AUFI), which is the most frequent reason for seeking healthcare services in Africa [6]. The World Health Organization (WHO) reported 263 million malaria cases across the globe with Africa accounting for 94% of the cases. The same reports indicated 597,000 deaths across the globe with Africa accounting for 95% of the deaths [7]. Dengue fever has also been in the rise in sub-Saharan Africa with around 200,000 suspected cases and 90,000 confirmed cases that resulted in 900 deaths [8] [9]. Most of the cases in Africa go unreported leading to inaccurate statistics.

One of the key challenges of the management of both diseases is misdiagnosis which is more prevalent in Africa due to the prevalence of both types of mosquitoes that spread the disease [5]. As a result, this clinical gap presents an opportunity for research in mathematical epidemiological modelling of malaria-dengue fever coinfection. Therefore, this study focused on developing a mathematical model that investigates the coinfection dynamics of the two diseases in one geographical area.

2. Model Description and Formulation

In this model, the total human population at any given time t, denoted by (N_h) is divided in ten human beings sub-classes. These are susceptible humans (S_h), individuals exposed to malaria (E_m), individuals infected by malaria (I_m), and individuals who recover from malaria (R_m). On the other side, we have individ-

uals exposed to dengue (E_d), individuals misdiagnosed (M_d), individuals infected by dengue (I_d), and individuals who recover from dengue (R_d). At the center of the model are individuals infected with malaria and dengue co-infection (I_c) and individuals who recover from malaria and dengue fever (R_c). Susceptible humans are those that are at risk of developing an infection. Infectious individuals are those that have symptoms of either of the disease or both disease. Exposed individuals are those that have been bitten by an infected mosquito but have not become infectious. Recovered are those that show temporal immunity. Co-infection are those individuals that are infected with both malaria and dengue fever. Total human population is represented by

$$N_h = S_h + E_d + M_d + I_d + E_m + I_m + I_c + R_d + R_m + R_c$$

A schematic presentation of the malaria dengue fever spread dynamics was presented in **Figure 1** below.

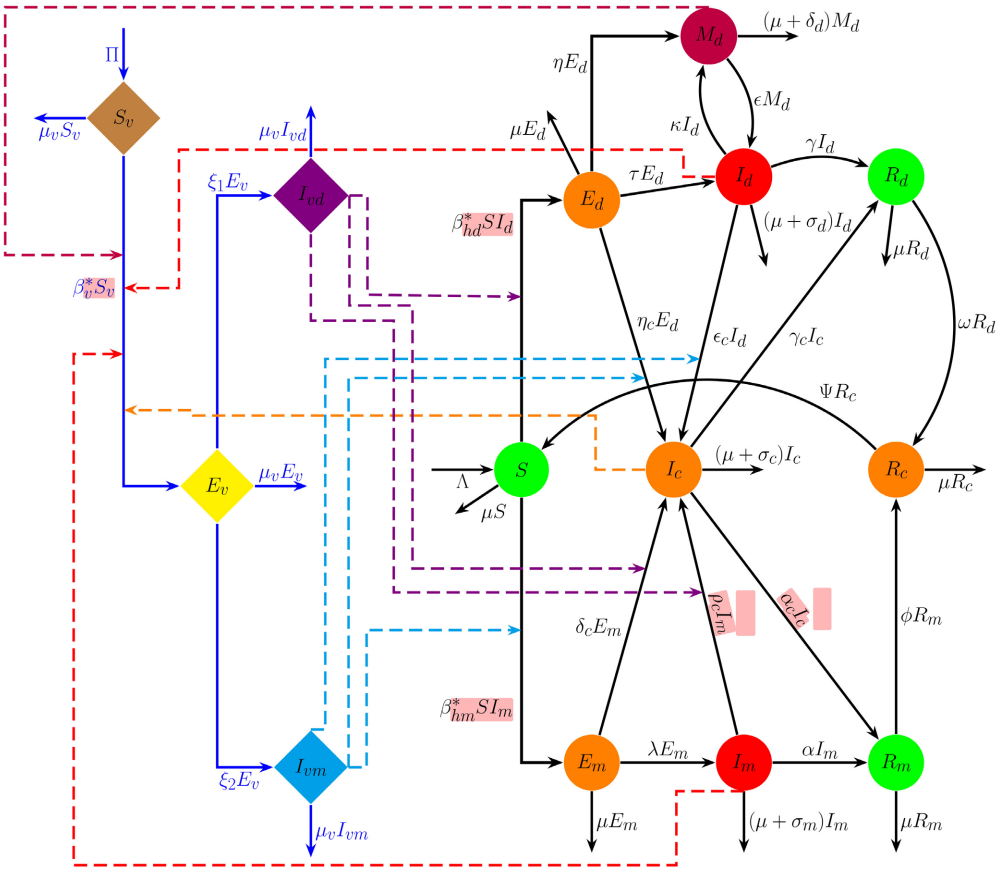

Figure 1. Malaria Dengue fever Coinfection model flow chart.

Susceptible are recruited through Λ, susceptibles individuals are exposed to dengue fever and malaria fever at rate of β_h^*, which is the force of infection. Individuals exposed to malaria fever move to infectious population at the rate of λ. Individuals exposed to dengue transfer to misdiagnosed population at rate of η. The misdiagnosed individuals transfer to infectious dengue individual at rate of

ε The exposed individuals to dengue move to infectious dengue population at rate of τ. Infectious dengue individuals move to misdiagnosis at rate of κ. Individuals infected by dengue and malaria fever move to co-infection human population at rate of ε_c and ρ_c respectively. Individuals exposed to dengue and malaria move to co-infection population at rate of η_c and δ_c respectively. Individual infected by dengue fever and malaria fever move to dengue recovered population and malaria recovered at rate of γ and α respectively.

Co-infected individuals move to dengue recovered and malaria recovered at rate of γ_c and α_c respectively. The recovered dengue and malaria individuals move to co-infected recovered at the rate of ω and ϕ respectively. individuals from co-infected recovered move to susceptible human population at rate of Ψ. Natural death rate in all compartment is μ. The diseases induced death rates for misdiagnosed individuals, infected dengue, co-infection and infected malaria are δ_d, σ_d, σ_c, σ_m respectively.

The vector population is divided into four compartments namely the susceptible vectors (S_v). The susceptible vectors entail the mosquitoes which are susceptible to both dengue virus and plasmodium bacteria. Mosquitoes that bite infected individuals proceed to the latent stage where they fit the description of an exposed compartment labelled (E_v). At this stage the dengue virus or the plasmodium bacteria has not replicated enough to make the mosquito to be infectious. When disease agent in the mosquito replicates to enough agents the mosquito can move to either the Infectious dengue mosquito compartment (I_{vd}) with mosquitoes infected with dengue fever, or moves to the infectious malaria compartment (I_{vm}) compartment for mosquitoes infected with plasmodium bacteria. The total vector population is given by $N_v = S_v + E_v + I_{vd} + I_{md}$.

The susceptible mosquitoes are recruited through natural hatching of eggs at the rate Π. The susceptible mosquitoes become infectious with either plasmodium or dengue fever through the force of infection β_v^* and thus move to the latent stage. The latent mosquitoes become infectious of dengue fever at a rate ξ_1 and become infectious with malaria at a rate ξ_2. All vectors in all compartments are susceptible to natural attrition at a rate of μ_v. A summary of the parameters is defined in Table 1 below.

Table 1. Numerical values for malaria-dengue Co-infection model parameters.

Param	Description	Value (day^{-1})	Reference
Λ	Human recruitment rate	0.00011	[10]
β^*	Force of infection rate	0.000035	[11]
η	rate of exposed dengue individuals transfer to misdiagnosed	0.00500	[12]
ε	rate of misdiagnosed individuals move to infectious human population	0.00200	[13]

Continued

λ	rate at which individuals exposed to malaria move to infectious malaria population	0.00100	[14]
τ	rate at which individual exposed to dengue move infectious dengue population	0.00142	[15]
κ	rate at which infectious dengue individuals move to misdiagnosis	0.00100	[12]
ε_c	rate of infectious dengue individuals moving to infectious co-infection	0.00020	[Estimated]
ρ_c	rate of infectious malaria individuals moving to infectious co-infection	0.00300	[Estimated]
η_c	rate of exposed dengue individuals move to infectious co-infection	0.00100	[Estimated]
δ_c	rate of exposed malaria individuals move to infectious co-infection	0.00100	[16]
γ	rate of recovered dengue individual from infectious dengue population	0.00142	[17]
α	rate of recovered malaria individuals from infectious malaria population	0.07100	[18]
γ_c	rate of dengue recovered individuals from co-infection	0.00125	[19]
α_c	rate of malaria recovered individuals from co-infection	0.00500	[20]
ω	rate of individual moving to co-infection recovered from dengue recovered	0.00100	[20]
ϕ	rate of individual moving to co-infection recovered from malaria recovered	0.00100	[19]
μ	rate of natural death rate	0.00004	[9]
δ_d	induced death rate for misdiagnosed	0.00200	[Estimated]
σ_d	disease induced death rate for dengue	0.00040	[21]
σ_c	diseases induced death rate for co-infection	0.00500	[22]
σ_m	disease induced death rate for malaria	0.00100	[21]

The force of infection for the coinfection model was taken to be $\beta_v^* = \beta_{vd}^* + \beta_{vm}^*$ where

$$\beta_{vd}^* = \frac{b_h \beta_{vhd} I_{hd}}{N_h}$$

where

b_h is the number of mosquito bites that one human has per unit time,

β_{vhd} is the dengue transmission rate from mosquitoes to human beings,

I_{hd} infected human beings with dengue fever.

and

$$\beta_{vm}^{*} = \frac{b_v T \beta_{hvm} I_{hm}}{N_h}$$

where

b_v is the number of human bites that one mosquito has per unit time,

β_{hvm} is the malaria transmission rate from mosquitoes to human beings,

T is the temperature coefficient of biting rate effectiveness given by $0 \le T \le 1$.

While the force of infection of the human population $\beta_h^{*} = \beta_{hm}^{*} + \beta_{hd}^{*}$, defined as

$$\beta_{hm}^{*} = \frac{b_h T \beta_{hvm} I_{vm}}{N_v}$$

where

b_h is the number of mosquito bites that one human has per unit time,

β_{hvm} is the malaria transmission rate from mosquitoes to human beings,

T is the temperature coefficient of biting rate effectiveness given by $0 \le T \le 1$.

and

$$\beta_{hd}^{*} = \frac{b_h \beta_{hvd} I_{vd}}{N_v} + \frac{b_h \theta M_{hd}}{N_h}$$

where

b_h is the number of mosquito bites that one human has per unit time,

β_{hvd} is the dengue transmission rate from human beings to mosquitoes,

θ infectiousness modifiers for misdiagnosis ($0 < \theta \le 1$),

I_{vd} dengue infected mosquitoes population,

M_{hd} Misdiagnosed human population.

2.1. Assumptions

The Model Utilized the Following Assumptions:

1) The population mixes homogeneously.

2) The parameters are uniform across all strata of population, therefore the biting rate of mosquitoes is uniform despite evidence of variation in mosquito preferences in biting.

3) There are no vertical transmissions of plasmodium.

4) There is no misdiagnosis of malaria due to the large number of malaria cases making health practitioners more proficient on malaria diagnosis.

5) There is no simultaneous recovery from both disease.

6) The contribution of the transmission of either disease by individuals co-infected is insignificant hence ignored.

2.2. Model Equations

The model description in **Figure 1** gives rise to a system of non-linear differential equations below that describe the malaria-dengue fever disease host-vector transmission dynamics.

$$\begin{cases} \dfrac{\mathrm{d}S}{\mathrm{d}t} = \Lambda - \beta^* S I_d - \beta^* S I_m - \mu S + \Psi R_c \\ \dfrac{\mathrm{d}E_d}{\mathrm{d}t} = \beta^* S I_d - (\mu + \eta_c + \eta + \tau) E_d \\ \dfrac{\mathrm{d}M_d}{\mathrm{d}t} = \eta E_d + \kappa I_d - \varepsilon M_d - (\mu + \delta_d) M_d \\ \dfrac{\mathrm{d}I_d}{\mathrm{d}t} = \tau E_d + \varepsilon M_d - \kappa I_d - (\mu + \sigma_d) I_d - \varepsilon_c I_d - \gamma I_d \\ \dfrac{\mathrm{d}R_d}{\mathrm{d}t} = \gamma I_d + \gamma_c I_c - \mu R_d - \omega R_d \\ \dfrac{\mathrm{d}E_m}{\mathrm{d}t} = \beta^* S I_m - \mu E_m - \lambda E_m - \delta_c E_m \\ \dfrac{\mathrm{d}I_m}{\mathrm{d}t} = \lambda E_m - \rho_c I_m - (\mu + \sigma_m) I_m - \alpha I_m \\ \dfrac{\mathrm{d}R_m}{\mathrm{d}t} = \alpha I_m + \alpha_c I_c - \Phi R_m - \mu R_m \\ \dfrac{\mathrm{d}I_c}{\mathrm{d}t} = \delta_c E_m + \rho_c I_m + \varepsilon_c I_d + \eta_c E_d - (\mu + \delta_c) I_c - \alpha_c I_c - \gamma_c I_c \\ \dfrac{\mathrm{d}R_c}{\mathrm{d}t} = \Phi R_m + \omega R_d - \mu R_c - \Psi R_c \\ \dfrac{\mathrm{d}S_v}{\mathrm{d}t} = \Pi - \mu_v S_v - \beta^* S_v \\ \dfrac{\mathrm{d}E_v}{\mathrm{d}t} = \beta_v^* S_v - \xi_1 E_v - \xi_2 E_v - \mu_v E_v \\ \dfrac{\mathrm{d}I_{vm}}{\mathrm{d}t} = \xi_2 E_v - \mu_v I_{vm} \\ \dfrac{\mathrm{d}I_{vd}}{\mathrm{d}t} = \xi_1 E_v - \mu_v I_{vd} \end{cases} \tag{1}$$

with the initial conditions

$$\begin{aligned} &S(0) \geq 0, E_d(0) \geq 0, M_d(0) \geq 0, I_d(0) \geq 0, R_d(0) \geq 0, E_m(0) \geq 0, I_m(0) \geq 0, \\ &R_m(0) \geq 0, I_c(0) \geq 0, R_c(0) \geq 0, S_v(0) \geq 0, E_v(0) \geq 0, I_{vm}(0) \geq 0, I_{vd}(0) \geq 0 \end{aligned} \tag{2}$$

3. Basic Properties of the Model

In this section, we study the posedness of the epidemiological model as stated by investigating the positivity and invariant region span by the model.

3.1. The Invariant Region

Theorem 1 Let's consider the space

$$\begin{aligned} \Xi_{MD} = \Big\{ &\big(S(t), E_d(t), M_d(t), I_d(t), R_d(t), E_m(t), I_m(t), R_m(t), I_c(t), R_c(t), \in \mathbb{R}_+^{10}\big): \\ &\big(S(t) > 0, E_d(t) > 0, M_d(t) \geq 0, I_d(t) \geq 0, R_d(t) \geq 0, E_m(t) > 0, I_m(t) \geq 0, \\ &R_m(t) \geq 0, I_c(t) \geq 0, R_c(t) \geq 0, S_v(t) \geq 0, E_v(t) \geq 0, I_{vm}(t) \geq 0, I_{vd}(t) \geq 0, \in \mathbb{R}_+^{14}\big)\Big\} \end{aligned} \tag{3}$$

then the solutions of $\big(S(t),\ E_d(t),\ M_d(t),\ I_d(t),\ R_d(t),\ E_m(t),\ I_m(t),\ R_m(t),\ I_c(t),\ R_c(t),\ S_v(t),\ E_v(t),\ I_{vm}(t),\ I_{vd}(t)\big)$ should be non-negative

for all time $t \geq 0$. Considering the fact that the initial conditions $\left(S(t) > 0,\ E_d(t) > 0,\ M_d(t) \geq 0,\ I_d(t) \geq 0,\ R_d(t) \geq 0,\ E_m(t) > 0,\ I_m(t) \geq 0,\ R_m(t) \geq 0,\ I_c(t) \geq 0,\ R_c(t) \geq 0,\ S_v(t) \geq 0,\ E_v(t) \geq 0,\ I_{vm}(t) \geq 0,\ I_{vd}(t) \geq 0\right)$ are non-negative, then the generation solutions $\left(S(t),\ E_d(t),\ M_d(t),\ I_d(t),\ R_d(t),\ E_m(t),\ I_m(t),\ R_m(t),\ I_c(t),\ R_c(t)\right)$ should be non-negative at any time $t \geq 0$.

Proof. We considered the total human population $N(t)$ at any given time t defined as

$$\begin{aligned} N(t) = S(t) + E_d(t) + M_d(t) + I_d(t) + R_d(t) \\ + E_m(t) + I_m(t) + R_m(t) + I_c(t) + R_c(t) \end{aligned} \tag{4}$$

differentiating both sides of Equation (4) we obtained

$$\begin{aligned} \frac{\mathrm{d}N(t)}{\mathrm{d}t} = \frac{\mathrm{d}S(t)}{\mathrm{d}t} + \frac{\mathrm{d}E_d(t)}{\mathrm{d}t} + \frac{\mathrm{d}M_d(t)}{\mathrm{d}t} + \frac{\mathrm{d}I_d(t)}{\mathrm{d}t} + \frac{\mathrm{d}R_d(t)}{\mathrm{d}t} \\ + \frac{\mathrm{d}E_m(t)}{\mathrm{d}t} + \frac{\mathrm{d}I_m(t)}{\mathrm{d}t} + \frac{\mathrm{d}R_m(t)}{\mathrm{d}t} + \frac{\mathrm{d}I_c(t)}{\mathrm{d}t} + \frac{\mathrm{d}R_c(t)}{\mathrm{d}t} \end{aligned} \tag{5}$$

In the event that there is no disease in the community then Equation (5) reduces to

$$\frac{\mathrm{d}N}{\mathrm{d}t} = \Lambda - \mu S - \mu E_d - \mu M_d - \mu I_d - \mu R_d - \mu E_m - \mu I_m - \mu R_m - \mu I_c - \mu R_c \tag{6}$$

which was further simplified to

$$N(t) \leq \frac{\Lambda}{\mu} - \left(\frac{\Lambda - \mu N(0)}{\mu}\right)\mathrm{e}^{-\mu t} \tag{7}$$

As $t \to \infty$ then $N(t) \to \frac{\Lambda}{\mu}$, which is the upper bound while zero is the lower bound of the population. As a consequence, the positive bounded region is expressed in the form in Equation (8) below

$$0 \leq N(t) \leq \frac{\Lambda}{\mu} \tag{8}$$

Therefore, the positive invariant region Π_h was found to be expressed as shown in the Equation (9) below

$$\begin{aligned} \Xi_h = \Big\{ \left(S(t), E_d(t), M_d(t), I_d(t), R_d(t), E_m(t), I_m(t), R_m(t), I_c(t), R_c(t), \in \mathbb{R}_+^{10}\right): \\ S(t) + E_d(t) + M_d(t) + I_d(t) + R_d(t) + E_m(t) + I_m(t) + R_m(t) + I_c(t) + R_c(t) \leq \frac{\Lambda}{\mu} \Big\} \end{aligned} \tag{9}$$

Considering the total vector population $N_v(t)$ at any given time t defined as

$$N_v(t) = S_v(t) + E_v(t) + I_{vd}(t) + I_{vm}(t) \tag{10}$$

differentiating both side Equation (10) with respect to time we obtained the following equation

$$\frac{\mathrm{d}N_v(t)}{\mathrm{d}t} = \frac{\mathrm{d}S_v(t)}{\mathrm{d}t} + \frac{\mathrm{d}E_v(t)}{\mathrm{d}t} + \frac{\mathrm{d}I_{vd}(t)}{\mathrm{d}t} + \frac{\mathrm{d}I_{vm}(t)}{\mathrm{d}t} \tag{11}$$

which was simplified as

$$N_v(t) \le \frac{\Pi}{\mu} - \left(\frac{\Pi - \mu N_v(0)}{\mu}\right) e^{-\mu t} \tag{12}$$

At $t \to t$ then $N_v \to \frac{\Pi}{\mu}$ with zero as the lower bound and $\frac{\Pi}{\mu}$ as the upper bound of the population. As a result the bounded region for the vector population is given by

$$0 \le N_v(t) \le \frac{\Pi}{\mu_v} \tag{13}$$

As a result the positive invariant region for the vector population was given by

$$\Xi_v = \left\{ \left(S_v(t), E_v(t), I_{vd}(t), I_{vm}(t), \in \mathbb{R}_+^4\right) : S_v(t) + E_v(t) + I_{vm}(t) + I_{vd}(t) \le \frac{\Pi_v}{\mu_v} \right\} \tag{14}$$

which is positively invariant region for the vector population □

In conclusion, the system of differential Equation (1) has solutions that are positively invariant in Ξ_h and Ξ_v [23] [24]. Therefore, the solutions of the system of differential equations that model the malaria-dengue fever coinfection are said to be well posed mathematically and epidemiologically well stated.

3.2. Co-Infection-Free Equilibrium

The disease free equilibrium was determined by considering the steady state of the spread dynamics [25]. At the steady state, the system is at its equilibrium point implying that the system does not change with respect to time [26]. Therefore, $\frac{\mathrm{d}}{\mathrm{d}t} = 0$ which implies that the left hand side of the system of differential equation in Equation (1) below is equated to zero to obtain.

$$\begin{aligned}
0 &= \Lambda - \beta^* S I_d - \beta^* S I_m - \mu S + \Psi R_c \\
0 &= \beta^* S I_d - (\mu + \eta_c + \eta + \tau) E_d \\
0 &= \eta E_d + \kappa I_d - \varepsilon M_d - (\mu + \delta_d) M_d \\
0 &= \tau E_d + \varepsilon M_d - \kappa I_d - (\mu + \sigma_d) I_d - \varepsilon_c I_d - \gamma I_d \\
0 &= \gamma I_d + \gamma_c I_c - \mu R_d - \omega R_d \\
0 &= \beta^* S I_m - \mu E_m - \lambda E_m - \delta_c E_m \\
0 &= \lambda E_m - \rho_c I_m - (\mu + \sigma_m) I_m - \alpha I_m \\
0 &= \alpha I_m + \alpha_c I_c - \Phi R_m - \mu R_m \\
0 &= \delta_c E_m + \rho_c I_m + \eta_c E_d - (\mu + \delta_c) I_c - \alpha_c I_c \\
0 &= \Phi R_m + \omega R_d - \mu R_c - \Psi R_c \\
0 &= \Pi - \mu_v S_v - \beta_v^* S_v \\
0 &= \beta_v^* S_v - \xi_1 E_v - \xi_2 E_v - \mu_v E_v \\
0 &= \xi_2 E_v - \mu_v I_{vm} \\
0 &= \xi_1 E_v - \mu_v I_{vd}
\end{aligned} \tag{15}$$

At the same time, at the disease free equilibrium, the disease does not exist in the community therefore, all the compartments associated with the disease are equated to zero. That is $E_d = 0$, $M_d = 0$, $I_d = 0$, $R_d = 0$, $E_m = 0$, $I_m = 0$,

$R_m = 0$, $I_c = 0$, $R_c = 0$, $E_v = 0$, $I_{vd} = 0$, $I_{vm} = 0$, as a consequence, the system of differential Equation (15) reduces to

$$0 = \Lambda - \mu S \tag{16}$$

Making S the subject and simplifying the equation we obtained

$$S = \frac{\Lambda}{\mu} \tag{17}$$

Again, considering the equation

$$0 = \Pi - \mu_v S_v \tag{18}$$

Making S_v the subject of the equation we obtained

$$S_v = \frac{\Pi}{\mu_v} \tag{19}$$

Therefore, the disease free equilibrium point can be summarized as follows

$$\begin{aligned} \xi_{03} &= \left(S^*, E_d^*, M_d^*, I_d^*, R_d^*, E_m^*, I_m^*, R_m^*, I_c^*, R_c^*, S_v^*, E_v^*, I_{vd}^*, I_{vm}^*\right) \\ &= \left(\frac{\Lambda}{\mu}, 0, 0, 0, 0, 0, 0, 0, 0, \frac{\Pi}{\mu_v}, 0, 0, 0\right) \end{aligned} \tag{20}$$

Therefore Equation (20) confirms the existence of the Co-infection-free equilibrium point of the system of differential Equation (1) that describe the malaria-dengue fever coinfection spread dynamics.

3.3. The Co-Infection Reproductive Number

The basic reproduction number is a critical dimensionless number that effectively describes the trajectory the coinfection will take in future [27]. It was calculated by separating the compartments into the infectious compartments and the non-infectious compartments. The non-infectious compartments in this study included (S, R_d, R_m, R_c, S_v) while the infectious compartments included $(E_d, M_d, I_d, E_m, I_m, I_c, E_v, I_{vm}, I_{vd})$. We then constructed the matrix of new infections F and the matrix of transfers V using the infectious compartments and obtained the results as follows

$$F = \begin{bmatrix} 0 & \frac{b_h\theta\Lambda}{\mu} & 0 & 0 & 0 & 0 & 0 & \frac{Tb_h\beta_{hm}\Lambda}{\mu} & \frac{b_h\beta_{hvd}\Lambda}{\mu} \\ 0 & 0 & 0 & 0 & 0 & 0 & 0 & 0 & 0 \\ 0 & 0 & 0 & 0 & 0 & 0 & 0 & 0 & 0 \\ 0 & \frac{b_h\theta\Lambda}{\mu} & 0 & 0 & 0 & 0 & 0 & \frac{Tb_h\beta_{hm}\Lambda}{\mu} & \frac{b_h\beta_{hvd}\Lambda}{\mu} \\ 0 & 0 & 0 & 0 & 0 & 0 & 0 & 0 & 0 \\ 0 & 0 & 0 & 0 & 0 & 0 & 0 & 0 & 0 \\ 0 & 0 & \frac{b_h\beta_{vhd}\Pi}{\mu_v} & 0 & \frac{Tb_v\beta_{hvm}\Pi}{\mu_v} & 0 & 0 & 0 & 0 \\ 0 & 0 & 0 & 0 & 0 & 0 & 0 & 0 & 0 \\ 0 & 0 & 0 & 0 & 0 & 0 & 0 & 0 & 0 \end{bmatrix} \tag{21}$$

and

$$V=\begin{bmatrix} k_1 & 0 & 0 & 0 & 0 & 0 & 0 & 0 & 0 \\ -\eta & k_2 & -\kappa & 0 & 0 & 0 & 0 & 0 & 0 \\ -\tau & -\varepsilon & k_3 & 0 & 0 & 0 & 0 & 0 & 0 \\ 0 & 0 & 0 & k_4 & 0 & 0 & 0 & 0 & 0 \\ 0 & 0 & 0 & -\lambda & k_5 & 0 & 0 & 0 & 0 \\ -\eta_c & 0 & 0 & -\delta_c & -\rho_c & k_6 & 0 & 0 & 0 \\ 0 & 0 & 0 & 0 & 0 & 0 & k_7 & 0 & 0 \\ 0 & 0 & 0 & 0 & 0 & 0 & -\xi_2 & k_8 & 0 \\ 0 & 0 & 0 & 0 & 0 & 0 & -\xi_1 & 0 & k_9 \end{bmatrix} \tag{22}$$

where

$$\begin{aligned} k_1 &= \mu+\eta_c+\eta+\tau, \\ k_2 &= \varepsilon+\mu+\delta_d, \\ k_3 &= \kappa+\mu+\sigma_d+\varepsilon_c+\gamma, \\ k_4 &= \mu+\lambda+\delta_c, \\ k_5 &= \rho_c+\mu+\sigma_m+\alpha, \\ k_6 &= \mu+\delta_c+\alpha_c, \\ k_7 &= \xi_1+\xi_2+\mu, \\ k_8 &= \mu_v, \quad k_9=\mu_v \end{aligned}$$

The next generation matrix was determined from the matrix $N=FV^{-1}$ which used to determine the basic reproduction number R_{0c}. We first determined the inverse of V in Equation (22). The inverse was determined as

$$V^{-1}=\begin{bmatrix} \frac{1}{k_1} & 0 & 0 & 0 & 0 & 0 & 0 & 0 & 0 \\ -\frac{\eta k_3+\kappa\tau}{k_1(\epsilon\kappa-k_3k_2)} & -\frac{k_3}{\epsilon\kappa-k_3k_2} & -\frac{\kappa}{\epsilon\kappa-k_3k_2} & 0 & 0 & 0 & 0 & 0 & 0 \\ -\frac{\epsilon\eta+\tau k_2}{k_1(\epsilon\kappa-k_3k_2)} & -\frac{\epsilon}{\epsilon\kappa-k_3k_2} & -\frac{k_2}{\epsilon\kappa-k_3k_2} & 0 & 0 & 0 & 0 & 0 & 0 \\ 0 & 0 & 0 & \frac{1}{k_4} & 0 & 0 & 0 & 0 & 0 \\ 0 & 0 & 0 & \frac{\lambda}{k_4k_5} & \frac{1}{k_5} & 0 & 0 & 0 & 0 \\ \frac{\eta_c}{k_1k_6} & 0 & 0 & \frac{\rho_c\lambda+\delta_ck_5}{k_5k_4k_6} & \frac{\rho_c}{k_5k_6} & \frac{1}{k_6} & 0 & 0 & 0 \\ 0 & 0 & 0 & 0 & 0 & 0 & \frac{1}{k_7} & 0 & 0 \\ 0 & 0 & 0 & 0 & 0 & 0 & \frac{\xi_2}{k_7k_8} & \frac{1}{k_8} & 0 \\ 0 & 0 & 0 & 0 & 0 & 0 & \frac{\xi_1}{k_7k_9} & 0 & \frac{1}{k_9} \end{bmatrix} \tag{23}$$

The matrix product FV^{-1} was obtained as

$$FV^{-1}=\begin{bmatrix} -\frac{b_h\theta\Lambda(\eta k_3+\kappa\tau)}{\mu k_1(\epsilon\kappa-k_3k_2)} & -\frac{b_h\theta\Lambda k_3}{\mu(\epsilon\kappa-k_3k_2)} & -\frac{b_h\theta\Lambda\kappa}{\mu(\epsilon\kappa-k_3k_2)} & 0 & 0 & 0 & \frac{Tb_h\beta_{hm}\Lambda\xi_2}{\mu k_7k_8}+\frac{b_h\beta_{hvd}\Lambda\xi_1}{\mu k_7k_9} & \frac{Tb_h\beta_{hm}\Lambda}{\mu k_8} & \frac{b_h\beta_{hvd}\Lambda}{\mu k_9} \\ 0 & 0 & 0 & 0 & 0 & 0 & 0 & 0 & 0 \\ 0 & 0 & 0 & 0 & 0 & 0 & 0 & 0 & 0 \\ -\frac{b_h\theta\Lambda(\eta k_3+\kappa\tau)}{\mu k_1(\epsilon\kappa-k_3k_2)} & -\frac{b_h\theta\Lambda k_3}{\mu(\epsilon\kappa-k_3k_2)} & -\frac{b_h\theta\Lambda\kappa}{\mu(\epsilon\kappa-k_3k_2)} & 0 & 0 & 0 & \frac{Tb_h\beta_{hm}\Lambda\xi_2}{\mu k_7k_8}+\frac{b_h\beta_{hvd}\Lambda\xi_1}{\mu k_7k_9} & \frac{Tb_h\beta_{hm}\Lambda}{\mu k_8} & \frac{b_h\beta_{hvd}\Lambda}{\mu k_9} \\ 0 & 0 & 0 & 0 & 0 & 0 & 0 & 0 & 0 \\ 0 & 0 & 0 & 0 & 0 & 0 & 0 & 0 & 0 \\ -\frac{b_h\beta_{vhd}\pi(\epsilon\eta+\tau k_2)}{\mu_v k_1(\epsilon\kappa-k_3k_2)} & -\frac{b_h\beta_{vhd}\pi\epsilon}{\mu_v(\epsilon\kappa-k_3k_2)} & -\frac{b_h\beta_{vhd}\pi k_2}{\mu_v(\epsilon\kappa-k_3k_2)} & \frac{Tb_v\beta_{hvm}\pi\lambda}{\mu_v k_4k_5} & \frac{Tb_v\beta_{hvm}\pi}{\mu_v k_5} & 0 & 0 & 0 & 0 \\ 0 & 0 & 0 & 0 & 0 & 0 & 0 & 0 & 0 \\ 0 & 0 & 0 & 0 & 0 & 0 & 0 & 0 & 0 \end{bmatrix} \tag{24}$$

whose eigenvalues were determined as follows

$$\lambda=\begin{bmatrix} 0 \\ 0 \\ 0 \\ 0 \\ 0 \\ 0 \\ 0 \\ 0 \\ \frac{-\frac{b_h\theta\Lambda(\eta k_3+\kappa\tau)}{\mu k_1(\epsilon\kappa-k_2k_3)}+\sqrt{\left(\frac{b_h\theta\Lambda(\eta k_3+\kappa\tau)}{\mu k_1(\epsilon\kappa-k_2k_3)}\right)^2+4\left(\frac{Tb_h\beta_{hm}\Lambda\xi_2}{\mu k_7k_8}+\frac{b_h\beta_{hvd}\Lambda\xi_1}{\mu k_7k_9}\right)\left(\frac{b_h\beta_{vhd}\Pi(\epsilon\eta+\tau k_2)}{\mu_v k_1(\epsilon\kappa-k_2k_3)}\right)}}{2} \\ \frac{-\frac{b_h\theta\Lambda(\eta k_3+\kappa\tau)}{\mu k_1(\epsilon\kappa-k_2k_3)}-\sqrt{\left(\frac{b_h\theta\Lambda(\eta k_3+\kappa\tau)}{\mu k_1(\epsilon\kappa-k_2k_3)}\right)^2+4\left(\frac{Tb_h\beta_{hm}\Lambda\xi_2}{\mu k_7k_8}+\frac{b_h\beta_{hvd}\Lambda\xi_1}{\mu k_7k_9}\right)\left(\frac{b_h\beta_{vhd}\Pi(\epsilon\eta+\tau k_2)}{\mu_v k_1(\epsilon\kappa-k_2k_3)}\right)}}{2} \end{bmatrix} \tag{25}$$

The basic reproduction number is given by the spectral radius of the eigenvalues in Equation (25) [27]. Therefore, the basic reproduction number was determined as

$$R_{0c}=\frac{-\frac{b_h\theta\Lambda(\eta k_3+\kappa\tau)}{\mu k_1(\epsilon\kappa-k_2k_3)}+\sqrt{\left(\frac{b_h\theta\Lambda(\eta k_3+\kappa\tau)}{\mu k_1(\epsilon\kappa-k_2k_3)}\right)^2+4\left(\frac{Tb_h\beta_{hm}\Lambda\xi_2}{\mu k_7k_8}+\frac{b_h\beta_{hvd}\Lambda\xi_1}{\mu k_7k_9}\right)\left(\frac{b_h\beta_{vhd}\Pi(\epsilon\eta+\tau k_2)}{\mu_v k_1(\epsilon\kappa-k_2k_3)}\right)}}{2} \tag{26}$$

3.4. Local Stability of the Co-Infection-Free Equilibrium

The stability of the disease free equilibrium is a vital analytical point in the spread dynamics of malaria and dengue coinfection. We utilized the jacobian approach to determine the stability.

Theorem 2. The Co-infection-Free Equilibrium (ξ_{03}) is locally asymptotically stable point of the dynamical system 1 whenever $R_{0c}<1$.

Proof. The jacobian approach required the determination of the partial differential of the system of differential Equation (1) with respect to each compartment [28]. The jacobian was determined to be

$$J=\begin{bmatrix}
-\beta_h I_d - I_m\beta_h - \mu & 0 & 0 & -\beta_h S & 0 & 0 & -\beta_h S & 0 & 0 & \Psi & 0 & 0 & 0 & 0\\
\beta_h I_d & -\mu-\eta_c-\eta-\tau & 0 & \beta_h S & 0 & 0 & 0 & 0 & 0 & 0 & 0 & 0 & 0 & 0\\
0 & \eta & -\epsilon-\mu-\delta_d & \kappa & 0 & 0 & 0 & 0 & 0 & 0 & 0 & 0 & 0 & 0\\
0 & \tau & \epsilon & -\kappa-\mu-\sigma_d-\varepsilon_c-\gamma_1 & 0 & 0 & 0 & 0 & 0 & 0 & 0 & 0 & 0 & 0\\
0 & 0 & 0 & \gamma_1 & -\mu-\omega & 0 & 0 & 0 & \gamma_c & 0 & 0 & 0 & 0 & 0\\
I_m\beta_h & 0 & 0 & 0 & 0 & -\lambda-\mu-\delta_c & \beta_h S & 0 & 0 & 0 & 0 & 0 & 0 & 0\\
0 & 0 & 0 & 0 & 0 & \lambda & -\rho_c-\mu-\sigma_m-\alpha & 0 & 0 & 0 & 0 & 0 & 0 & 0\\
0 & 0 & 0 & 0 & 0 & 0 & \alpha & -\mu-\phi & \alpha_c & 0 & 0 & 0 & 0 & 0\\
0 & \eta_c & 0 & 0 & 0 & \delta_c & \rho_c & 0 & -\mu-\delta_c-\alpha_c & 0 & 0 & 0 & 0 & 0\\
0 & 0 & 0 & 0 & \omega & 0 & 0 & \phi & 0 & -\Psi-\mu & 0 & 0 & 0 & 0\\
0 & 0 & 0 & 0 & 0 & 0 & 0 & 0 & 0 & 0 & -\beta_v-\mu_v & 0 & 0 & 0\\
0 & 0 & 0 & 0 & 0 & 0 & 0 & 0 & 0 & 0 & \beta_v & -\mu_v-\xi_2 & 0 & 0\\
0 & 0 & 0 & 0 & 0 & 0 & 0 & 0 & 0 & 0 & 0 & \xi_2 & -\mu_v & 0\\
0 & 0 & 0 & 0 & 0 & 0 & 0 & 0 & 0 & 0 & 0 & \xi_1 & 0 & -\mu_v
\end{bmatrix} \tag{27}$$

where

$$k_1=\mu+\eta_c+\eta+\tau,\ k_2=\varepsilon+\mu+\delta_d,\ k_3=\kappa+\mu+\sigma_d+\varepsilon_c+\gamma,\ k_4=\mu+\omega,$$
$$k_5=\mu+\lambda+\delta_c,\ k_6=\rho_c+\mu+\sigma_m+\alpha,\ k_7=\Phi+\mu,\ k_8=\mu+\delta_c+\alpha_c,\ k_9=\mu+\Psi$$

Determining the jacobian at the disease free equilibrium $J_{\xi_{03}}$ we obtained

$$J_{\xi_{03}}=\begin{bmatrix}
-\mu & 0 & 0 & -\beta_h\frac{\Lambda}{\mu} & 0 & 0 & -\beta_h\frac{\Lambda}{\mu} & 0 & 0 & \Psi & 0 & 0 & 0 & 0\\
0 & -k_1 & 0 & \beta_h\frac{\Lambda}{\mu} & 0 & 0 & 0 & 0 & 0 & 0 & 0 & 0 & 0 & 0\\
0 & \eta & -k_2 & \kappa & 0 & 0 & 0 & 0 & 0 & 0 & 0 & 0 & 0 & 0\\
0 & \tau & \epsilon & -k_3 & 0 & 0 & 0 & 0 & 0 & 0 & 0 & 0 & 0 & 0\\
0 & 0 & 0 & \gamma & -k_4 & 0 & 0 & 0 & \gamma_c & 0 & 0 & 0 & 0 & 0\\
0 & 0 & 0 & 0 & 0 & -k_5 & \beta_h\frac{\Lambda}{\mu} & 0 & 0 & 0 & 0 & 0 & 0 & 0\\
0 & 0 & 0 & 0 & 0 & \lambda & -k_6 & 0 & 0 & 0 & 0 & 0 & 0 & 0\\
0 & 0 & 0 & 0 & 0 & 0 & \alpha & -k_7 & \alpha_c & 0 & 0 & 0 & 0 & 0\\
0 & \eta_c & 0 & 0 & 0 & \delta_c & \rho_c & 0 & -k_8 & 0 & 0 & 0 & 0 & 0\\
0 & 0 & 0 & 0 & \omega & 0 & 0 & \phi & 0 & -k_9 & 0 & 0 & 0 & 0\\
0 & 0 & 0 & 0 & 0 & 0 & 0 & 0 & 0 & 0 & -\mu_v & 0 & 0 & 0\\
0 & 0 & 0 & 0 & 0 & 0 & 0 & 0 & 0 & 0 & 0 & -\mu_v & 0 & 0\\
0 & 0 & 0 & 0 & 0 & 0 & 0 & 0 & 0 & 0 & 0 & \xi_2 & -\mu_v & 0\\
0 & 0 & 0 & 0 & 0 & 0 & 0 & 0 & 0 & 0 & 0 & \xi_1 & 0 & -\mu_v
\end{bmatrix} \tag{28}$$

Analyzing the jacobian matrix at DFE to determine the condition under which the DFE is locally asymptotically stable. The disease free equilibrium is locally asymptotically stable if all the eigenvalues of the jacobian matrix are negative. In Equation (28), it is clear that the first five eigenvalues are strictly negative. Considering the sub blocks of the coinfection and using the Routh-Hurwitz criterion for characteristic polynomials, we determined that the characteristic polynomial was established to be $P_2(\lambda)=\lambda^2+B_1\lambda+B_0=0$ where $B_1=k_5+k_6$ and $B_0=k_5k_6(1-R_{0m})$. According to Routh-Hurwitz criterion for quadratic characteristic polynomials $B_0>0$ which is true since both k_5 and k_6 are positive while $B_0>0$ whose positivity is dependent on the value of $(1-R_{0m})$ which is positive only when ($R_{0m}<1$) for local stability to be achieved. Considering the dengue infectious compartments, we determined that the characteristic polynomial is given by $P_1(\lambda)=\lambda^3+A_2\lambda^2+A_1\lambda+A_0=0$. The third-order Ruoth-Huwirtz criterion requires that $A_2>0$, $A_0>0$, $A_2A_1>A_0$. From the matrix $A_2=k_1+k_2+k_3>0$

since k_1, k_2 and k_3 are all positive. $A_0 = k_1\left(k_2k_3 - \varepsilon\kappa\right)\left(1 - R_{0d}\right)$ which is positive only if $R_{0d} < 1$. The third condition is met by expansion which is proven based on the biological constraints. As a consequence the diseases free equilibrium is locally asymptotically stable when all the described conditions are met. Considering the vector population, all the diagonals are represented by the parameter $-\mu_v$ thus making the eigenvalues of the vector population all negative thus making the disease free asymptotically stable.

3.5. Endemic Equilibrium

The endemic equilibrium is a steady state that exists when the disease is persistent in the community [29]. The system does not change with respect to time at this steady state implying that $\frac{\mathrm{d}}{\mathrm{d}t} = 0$. Considering the system of differential Equation (1) the endemic equilibrium was obtained as

$$\xi^{**} = \begin{pmatrix} S^{**} \\ E_d^{**} \\ M_d^{**} \\ I_d^{**} \\ R_d^{**} \\ E_m^{**} \\ I_m^{**} \\ R_m^{**} \\ I_c^{**} \\ R_c^{**} \\ S_v^{**} \\ E_v^{**} \\ I_{vd}^{**} \\ I_{vm}^{**} \end{pmatrix} = \begin{pmatrix} \dfrac{S^{**}}{R_{0c}^{**}} \\ \dfrac{\beta^* S^{**} I_d^{**} z}{k_1} \\ \dfrac{\eta E_d^* + \kappa I_d^{**}}{k_2} \\ \dfrac{\tau E_d^{**} + \varepsilon M_d^{**}}{k_3} \\ \dfrac{\gamma I_d^{**} + \gamma_c I_c^{**}}{k_4} \\ \dfrac{\beta^* S^* I_m^{**}}{k_5} \\ \dfrac{\lambda E_m^{**}}{k_6} \\ \dfrac{\alpha I_m^{**} + \alpha_c I_c^{**}}{k_7} \\ \dfrac{\delta_c E_m^{**} + \rho_c I_m^{**} + \eta_c E_d^{**}}{k_8} \\ \dfrac{\Phi R_m^{**} + \omega R_d^{**}}{k_9} \\ \dfrac{\Pi}{\mu_v + \beta_v^*} \\ \dfrac{\beta_v^* \Pi}{\left(\mu_v + \beta_v^*\right)\left(\xi_1 + \xi_2 + \mu_v\right)} \\ \dfrac{\xi_1 \beta_v^* \Pi}{\mu_v\left(\mu_v + \beta_v^*\right)\left(\xi_1 + \xi_2 + \mu_v\right)} \\ \dfrac{\xi_2 \beta_v^* \Pi}{\mu_v\left(\mu_v + \beta_v^*\right)\left(\xi_1 + \xi_2 + \mu_v\right)} \end{pmatrix} \tag{29}$$

where

$$k_1 = \mu + \eta_c + \eta + \tau, \quad k_2 = \varepsilon + \mu + \delta_d, \quad k_3 = \kappa + \mu + \sigma_d + \varepsilon_c + \gamma,$$
$$k_4 = \mu + \omega, \quad k_5 = \mu + \lambda + \delta_c, \quad k_6 = \rho_c + \mu + \sigma_m + \alpha,$$
$$k_7 = \Phi + \mu, \quad k_8 = \mu + \delta_c + \alpha_c, \quad k_9 = \mu + \Psi$$

3.6. Numerical Simulations

In this section, the spread dynamics of malaria and dengue fever were further analysed numerically to determine the spread dynamics patterns.

3.7. Sensitivity Indices

This section focused on determining the most sensitive parameter of the basic reproduction number. It utilised the numerical values in Table 1 and normalized forwards sensitivity index formula to obtain the values of Table 2 below.

Table 2. Sensitivity indices of the model parameters.

Parameter	Description	Sensitivity Index
Λ	Human recruitment rate	+1.000001
θ	Probability of infection at the misdiagnosed compartment	+1.000003
b_h	Biting rate per human	+1.000000
κ	Infectious dengue moving to misdiagnosis	+0.503391
η	Exposed dengue moving to misdiagnosis	+0.473991
ξ_2	Incubation rate of malaria	$+4.962018 \times 10^{-7}$
μ_v	Natural death rate for vectors	$+1.367197 \times 10^{-6}$
Π	Vector recruitment rate	-1.367197×10^{-6}
β_{vhd}	Transmission rate (vector to human)	-1.367197×10^{-6}
β_{hvd}	Transmission rate (human to vector)	-1.179910×10^{-6}
ξ_1	incubation rate of dengue fever	-4.964206×10^{-7}
T	the temperature coefficient of biting rate effectiveness	-1.872872×10^{-7}
β_{hm}	Transmission rate for malaria	-1.872872×10^{-7}
σ_d	Disease induced death rate (dengue)	−0.000185
δ_d	Induced death rate (misdiagnosed)	−0.003129
ε_c	Infectious dengue moving to co-infection	−0.013702
η_c	Exposed dengue moving to co-infection	−0.026120
τ	Progression to infectious dengue	−0.447610
γ	Recovery from infectious dengue	−0.489365
ε	Misdiagnosed moving to infectious	−0.994788
μ	Natural death rate	−1.002485

3.8. Numerical Coinfection Spread Dynamics

Table 1 above was utilized together with the following initial conditions $S(0)=99800$, $E_d(0)=50$, $M_d(0)=0$, $I_d(0)=50$, $R_d(0)=0$, $E_m(0)=50$, $I_m(0)=50$, $R_m(0)=0$, $I_c(0)=0$, $R_c(0)=0$ and the total population given by $N(t)=S(t)+E_d(t)+M_d(t)+I_d(t)+R_d(t)+E_m(t)+I_m(t)+R_m(t)+I_c(t)+R_c(t)$, to generate graphs for the spread dynamics. A total population of 100,000 people was considered because it mirrors a closed community which is scalable to national level population [30]. The numerical analysis was conducted by utilization of the Maple software. The spread dynamics of each of the compartment was show in Figure 2 below.

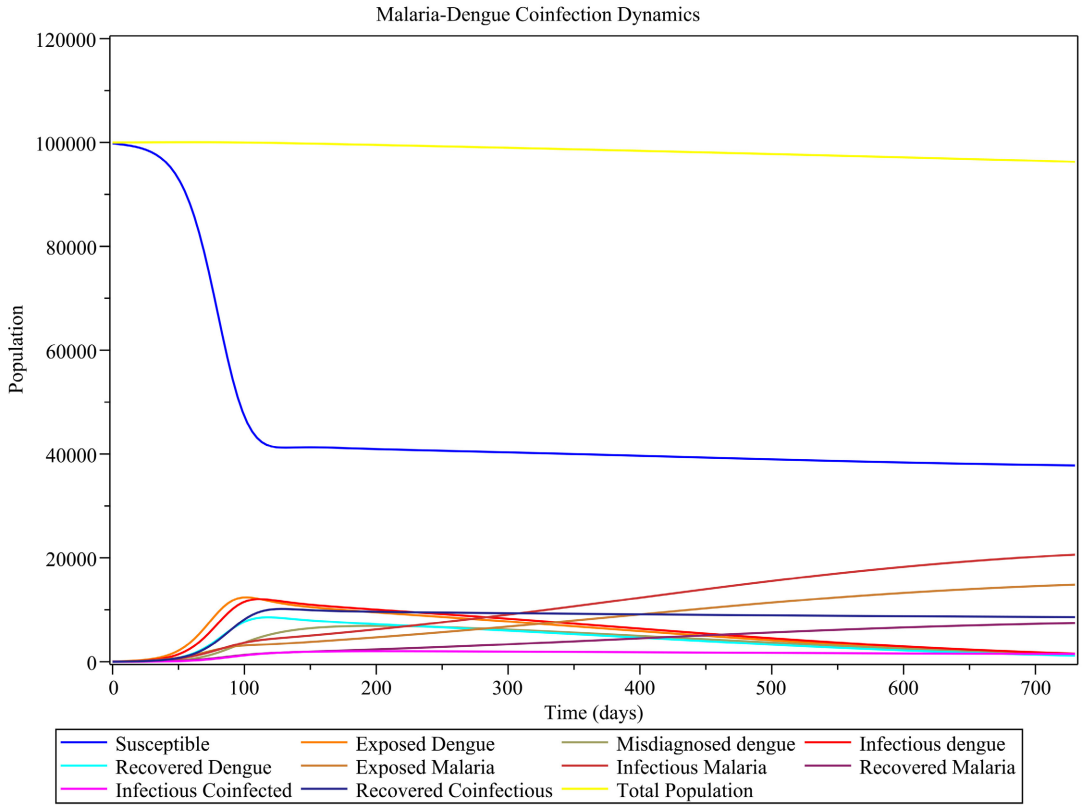

Figure 2. Numerical simulation of the general spread dynamics of malaria dengue coinfection.

The susceptible population remains high in the first 50 days of the study ans then decreased rapidly in the next 50 days due to the diseases gaining traction in the community. The susceptible population stabilizes at around 40,000 people per day implying that about 40,000 never get to interact with the diseases during the break out. The total population suffers a gentle decline over the 730 days of the study due to exit of people through disease related attrition. The spread dynamics of the other compartments were better illustrated by Figure 3.

Figure 3 gives a closeup of the spread dynamics the other compartments. Some of the defining aspects of the spread dynamics include: The spread dynamics of dengue fever take a short period of about 100 days to gain traction in the commu-

nity while the spread dynamics of malaria take a considerable long period to grain traction. The spread dynamics of dengue fever increase rapidly to reach a peak over a short period of time, while the decrease occurs gradually over a long period of time. The coinfected population raises to a stable population of about 3000 people per day. The population of coinfected individuals remains low but steady thus making it an point of concern for the containment of the diseases.

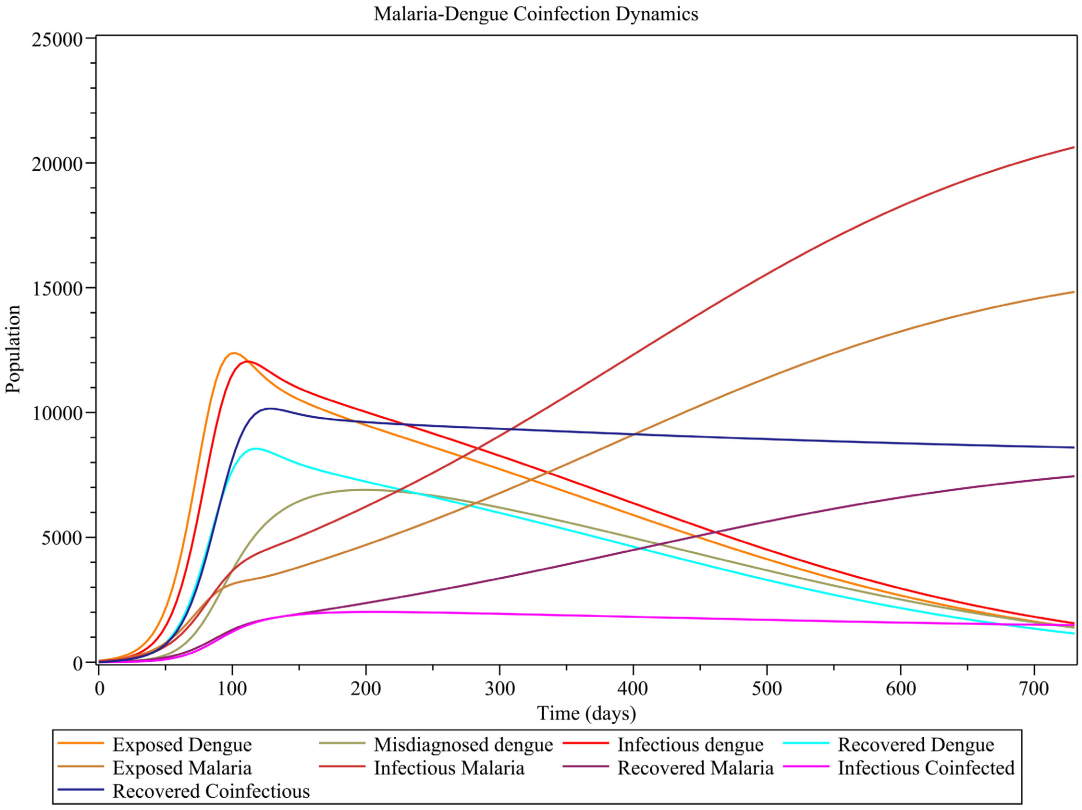

Figure 3. A close view of numerical simulation of the general spread dynamics of malaria dengue coinfection.

4. Conclusions and Recommendation

Malaria-dengue fever is an emerging public health concern among sub-Saharan Africa. This study has investigated the impact of misdiagnosis on the spread dynamics of the coinfection by developing and analysing a mathematical epidemiological model that describes the spread dynamics. The basic properties have been discussed and the model confirmed to be mathematically well stated and biologically well posed. The critical spread dynamics indicator such as the basic reproduction number has been determined. The behaviour of solutions has been determined through determining the existence of equilibrium points and their stabilities. The sensitivity indices have been determined to scout for the parameters that should be targeted for effective management of the spread dynamics. The study identified the biting rate, the human recruitment rate, the probability of infection by the misdiagnosed individuals, the natural death rate, and the rate of misdiagnosis as the most sensitive parameters. These parameters are the best candidates

to develop measures against, for effective management of malaria-dengue fever spread dynamics.

The study recommends the development of an optimal control solution of the spread dynamics to explore the best strategies of controlling the diseases. It also recommends developing the most sensitive parameters into functions to determine the critical levels for which the parameters can be managed to in a resource scarce economy. It also recommends collection of raw data to investigate the extent to which the coinfection has invaded communities.

Author Contributions

Conceptualization, Ewesit EW; methodology, Ewesit EW; software, Ewesit EW; validation, Ewesit EW, Wainaina M and Maingi D; formal analysis, Ewesit EW; investigation, Ewesit EW; resources, Ewesit EW; data curation, Ewesit EW; writing-original draft preparation, Ewesit EW; writing-review and editing, Ewesit EW; visualization, Ewesit EW; supervision, Wainaina M and Maingi D; project administration, Wainaina M and Maingi D; funding acquisition, Ewesit EW. All authors have read and agreed to the published version of the manuscript.

Conflicts of Interest

The authors declare no conflicts of interest regarding the publication of this paper.

References

[1] Epelboin, L., Hanf, M., Dussart, P., Ouar-Epelboin, S., Djossou, F., Nacher, M., *et al.* (2012) Is Dengue and Malaria Co-Infection More Severe than Single Infections? A Retrospective Matched-Pair Study in French Guiana. *Malaria Journal*, **11**, Article No. 142. https://doi.org/10.1186/1475-2875-11-142

[2] Bygbjerg, I.C., Simonsen, L. and Schiøler, K.L. (2018) Elimination of Falciparum Malaria and Emergence of Severe Dengue: An Independent or Interdependent Phenomenon? *Frontiers in Microbiology*, **9**, Article 1120. https://doi.org/10.3389/fmicb.2018.01120

[3] Wiwanitkit, V. (2011) Concurrent Malaria and Dengue Infection: A Brief Summary and Comment. *Asian Pacific Journal of Tropical Biomedicine*, **1**, 326-327. https://doi.org/10.1016/s2221-1691(11)60053-1

[4] Katzelnick, L.C., Gresh, L., Halloran, M.E., Mercado, J.C., Kuan, G., Gordon, A., *et al.* (2017) Antibody-Dependent Enhancement of Severe Dengue Disease in Humans. *Science*, **358**, 929-932. https://doi.org/10.1126/science.aan6836

[5] Gebremariam, T.T., Schallig, H.D.F.H., Kurmane, Z.M. and Danquah, J.B. (2023) Increasing Prevalence of Malaria and Acute Dengue Virus Coinfection in Africa: A Meta-Analysis and Meta-Regression of Cross-Sectional Studies. *Malaria Journal*, **22**, Article No. 300. https://doi.org/10.1186/s12936-023-04723-y

[6] Saady, M., Ewaisha, R. and Azzazy, H.M.E. (2025) Regional Burden of Undifferentiated Fever and Leading Infectious Etiologies of Acute Febrile Illness in Low- and Middle-Income Countries: A Meta-Analysis. *International Journal of Infectious Diseases*, **161**, Article 108152. https://doi.org/10.1016/j.ijid.2025.108152

[7] Yitageasu, G., Worede, E.A., Alemu, E.A., Tigabie, M., Birhanu, A., Angelo, A.A., *et al.* (2025) Malaria Prevalence and Its Determinants across 19 Sub-Saharan African

Countries: A Spatial and Geographically Weighted Regression Analysis. *Malaria Journal*, **24**, Article No. 305. https://doi.org/10.1186/s12936-025-05573-6

[8] Mwanyika, G.O., Moir, M., Musa, A.O., Poongavanan, J., Dor, G., Wilkinson, E., *et al.* (2025) A Decade of Dengue Disease Burden in Africa (2013-2023): A Systematic Review. *Travel Medicine and Infectious Disease*, **67**, Article 102897. https://doi.org/10.1016/j.tmaid.2025.102897

[9] Nyanaro, B., Kimathi, G. and Wainaina, M. (2024) Mathematical Modelling of Dengue Fever Transmission Dynamics in Kenya. *Journal of Applied Math*, **2**, Article 1807. https://doi.org/10.59400/jam1807

[10] Aguiar, M., Anam, V., Blyuss, K.B., Estadilla, C.D.S., Guerrero, B.V., Knopoff, D., *et al.* (2022) Mathematical Models for Dengue Fever Epidemiology: A 10-Year Systematic Review. *Physics of Life Reviews*, **40**, 65-92. https://doi.org/10.1016/j.plrev.2022.02.001

[11] Puspita, J.W., Fakhruddin, M., Nuraini, N. and Soewono, E. (2022) Time-Dependent Force of Infection and Effective Reproduction Ratio in an Age-Structure Dengue Transmission Model in Bandung City, Indonesia. *Infectious Disease Modelling*, **7**, 430-447. https://doi.org/10.1016/j.idm.2022.07.001

[12] Butt, A.I.K., Imran, M., McKinney, B.A., Batool, S. and Aftab, H. (2023) Mathematical and Stability Analysis of Dengue-Malaria Co-Infection with Disease Control Strategies. *Mathematics*, **11**, Article 4600. https://doi.org/10.3390/math11224600

[13] Adom-Konadu, A., Yankson, E., Naandam, S.M. and Dwomoh, D. (2022) A Mathematical Model for Effective Control and Possible Eradication of Malaria. *Journal of Mathematics*, **2022**, Article 6165581. https://doi.org/10.1155/2022/6165581

[14] Alhaj, M.S. (2023) Mathematical Model for Malaria Disease Transmission. *Journal of Mathematical Analysis and Modeling*, **4**, 1-16. https://doi.org/10.48185/jmam.v4i1.688

[15] Khan, M.A. and Fatmawati (2021) Dengue Infection Modeling and Its Optimal Control Analysis in East Java, Indonesia. *Heliyon*, **7**, e06023. https://doi.org/10.1016/j.heliyon.2021.e06023

[16] Duru, E.C., Mbah, G.C.E., Anyanwu, M.C. and Nnamani, N.T. (2024) Modelling the Co-Infection of Malaria and Zika Virus Disease. *Journal of the Nigerian Society of Physical Sciences*, **6**, Article 1938. https://doi.org/10.46481/jnsps.2024.1938

[17] Tan, L.K., Low, S.L., Sun, H., Shi, Y., Liu, L., Lam, S., *et al.* (2019) Force of Infection and True Infection Rate of Dengue in Singapore: Implications for Dengue Control and Management. *American Journal of Epidemiology*, **188**, 1529-1538. https://doi.org/10.1093/aje/kwz110

[18] Duve, P., Charles, S., Munyakazi, J., Lühken, R. and Witbooi, P. (2024) A Mathematical Model for Malaria Disease Dynamics with Vaccination and Infected Immigrants. *Mathematical Biosciences and Engineering*, **21**, 1082-1109. https://doi.org/10.3934/mbe.2024045

[19] Imran, M., McKinney, B.A., Butt, A.I.K., Palumbo, P., Batool, S. and Aftab, H. (2024) Optimal Control Strategies for Dengue and Malaria Co-Infection Disease Model. *Mathematics*, **13**, Article 43. https://doi.org/10.3390/math13010043

[20] Prakash Raj, M., Venkatesh, A., Arun Kumar, K. and Manivel, M. (2025) Mathematical Modeling of the Co-Infection Dynamics of Dengue and Malaria Using Delay Differential Equations. *Advanced Theory and Simulations*, **8**, Article 2400609. https://doi.org/10.1002/adts.202400609

[21] Harshit and Harjule, P. (2024) Mathematical Modelling and Analysis of Dengue

Transmission Dynamics. *Procedia Computer Science*, **235**, 539-548. https://doi.org/10.1016/j.procs.2024.04.053

[22] Kotepui, M., Kotepui, K.U., Milanez, G.D.J. and Masangkay, F.R. (2020) Prevalence of and Risk Factors for Severe Malaria Caused by Plasmodium and Dengue Virus Co-Infection: A Systematic Review and Meta-Analysis. *Infectious Diseases of Poverty*, **9**, Article No. 134. https://doi.org/10.1186/s40249-020-00741-z

[23] Nyasagare, B.N., Osman, S. and Wainaina, M. (2019) Modelling and Analysis of Campylobacteriosis in Human and Animal Populations. *Global Journal of Pure and Applied Mathematics*, **15**, 551-567.

[24] Onsongo, W.M., Mwini, E.D., Nyanaro, B.N. and Osman, S. (2022) Stability Analysis and Modelling the Dynamics of Psittacosis in Human and Poultry Populations. *Communications in Mathematical Biology and Neuroscience*, **2022**, Article 9.

[25] Eyaran, W.E., Osman, S. and Wainaina, M. (2019) Modelling and Analysis of SEIR with Delay Differential Equation. *Global Journal of Pure and Applied Mathematics*, **15**, 365-382.

[26] Onsongo, W.M., Mwini, E.D., Nyanaro, B.N. and Osman, S. (2021) The Dynamics of Psittacosis in Human and Poultry Populations: A Mathematical Modelling Perspective. *Journal of Mathematics and Computer Science*, **11**, 8472-8505.

[27] Muia, D.W., Osman, S. and Wainaina, M. (2018) Modelling and Analysis of Trypanosomiasis Transmission Mechanism. *Global Journal of Pure and Applied Mathematics*, **14**, 1311-1331.

[28] Osman, S., Otoo, D. and Sebil, C. (2020) Analysis of Listeriosis Transmission Dynamics with Optimal Control. *Applied Mathematics*, **11**, 712-737. https://doi.org/10.4236/am.2020.117048

[29] Osman, S., Otoo, D. and Makinde, O.D. (2020) Modeling Anthrax with Optimal Control and Cost Effectiveness Analysis. *Applied Mathematics*, **11**, 255-275. https://doi.org/10.4236/am.2020.113020

[30] Kretzschmar, M. and Wallinga, J. (2009) Mathematical Models in Infectious Disease Epidemiology. In: *Statistics for Biology and Health*, Springer, 209-221. https://doi.org/10.1007/978-0-387-93835-6_12